Talanta 81 (2010) 959–966

Contents lists available at ScienceDirect

Talanta

journal homepage: www.elsevier.com/locate/talanta

Tuning of the vinyl groups' spacing at surface of modified silica in preparation of high density imprinted layer-coated silica nanoparticles: A dispersive solid-phase extraction materials for chlorpyrifos

Qing Lu[a], Xuemei Chen[a], Li Nie[a], Jing Luo[a], Huijun Jiang[a], Lina Chen[a], Qin Hu[a], Shuhu Du[a,*], Zhongping Zhang[b]

[a] School of Pharmacy, Nanjing Medical University, Nanjing 210029, China
[b] Institute of Intelligent Machines, Chinese Academy of Sciences, Hefei, Anhui 230031, China

ARTICLE INFO

Article history:
Received 4 November 2009
Received in revised form 16 January 2010
Accepted 20 January 2010
Available online 25 January 2010

Keywords:
Molecular imprinting
Modified silica nanoparticles
Grafting to
Dispersive solid-phase extraction
Phosphate pesticides

ABSTRACT

This paper reports the preparation of high density imprinted layer-coated silica nanoparticles toward selective recognition and fast enrichment of chlorpyrifos (CP) from complicated matrices. The molecularly imprinted polymers (MIPs) were successfully coated at the surface of modified silica through using the chemical immovable vinyl groups at the nanoparticles' surface, followed by the graft copolymerization of methacrylic acid (MAA) and ethylene glycol dimethacrylate (EGDMA) in the presence of templates CP. It has been demonstrated that the space of end vinyl groups at the surface of silica can be controlled by changing the condition of chemical modification, regulating the thickness of imprinted shells and the density of efficient imprinted sites. After removal of templates by solvent extraction, the recognition sites of CP were created in the polymer coating layer. The CP-imprinted nanoparticles exhibited high recognition selectivity and binding affinity to CP analyte. When the CP-imprinted nanoparticles were used as dispersive solid-phase extraction (dSPE) materials, the high recovery yields of 76.1–93.5% from various spiked samples with only 1 μg/mL analyte were achieved by one-step extraction. These results reported herein provide the possibility for the separation and enrichment of CP from complicated matrices by the molecular imprinting modification at the surface of common silica nanoparticles.

1. Introduction

Organophosphates (OPs) such as chlorpyrifos (CP), which are known to be highly neurotoxic, can disrupt the cholinesterase enzyme that regulates acetylcholine [1–4], so they are widely used as pesticides. Due to their wide use and non-standard operation, OPs residuals in crop, vegetable, and poultry products are dangerous to human health. Therefore, it is quite necessary to detect OPs residuals in the food. Current measurement of OPs levels mainly rely on gas chromatography (GC) or high performance liquid chromatography (HPLC) method [5,6], which are usually of low efficiency due to the lack of specific adsorptive materials. Meanwhile, low concentration of OPs makes their analysis more difficult when traditional adsorbents were used in HPLC for their quantification. Moreover, the complicated matrices can seriously interfere with the enrichment of OPs residues to reduce the reliability and repetition of OPs analysis. Thus, the development of stable antibody-like materials with specific binding properties may make effective enrichment and selective detection of trace OPs pesticides possible.

Molecular imprinting technique can create specific molecular recognition sites in polymer matrix [7–12], offering the advanced sensitivity to target species as compared with traditional solid-phase extraction adsorbents [13–15]. The synthesis of MIPs involves the formation of the template–monomer complexes through either covalent or noncovalent interactions, followed by a copolymerization with excess cross-linking agent. Upon removal of templates from the cross-linked matrix generates the recognition cavities complementary to the shape, size, and functionality of templates. Thus, MIPs have specific molecular recognition ability and high binding affinity [16–18] to the template molecules, and are desired as adsorbents for selective recognition and enrichment the target molecules.

While various imprinted materials were made, these efforts have met with many limitations including incomplete template removal, small binding capacity, low affinity and irregular materials' shape. Currently, a molecular imprinting technique, surface-imprinting at silica adsorbents, has emerged, which greatly enhanced the efficiency of molecular imprinting [19–27]. Generally, the surface-imprinting processes could be carried out either

* Corresponding author.
E-mail addresses: shuhudu@njmu.edu.cn (S. Du), zpzhang@iim.ac.cn (Z. Zhang).

0039-9140/$ – see front matter.
doi:10.1016/j.talanta.2010.01.044

by the "grafting from" or "grafting to" methods. In the "grafting from" technique, the initiating groups were immobilized at the surfaces of nanoparticles. During polymerization, the grafting MIPs were propagated from the surface of the solid support by the various mechanisms including atom transfer radical polymerization (ATRP), reversible addition–fragmentation chain transfer (RAFT) and nitroxide-mediated processes (NMP) [28–31]. Though "grafting from" can produce a high grafting density on the surface of support due to the highly selective occurrence of polymerization, the process involves in a complicated chemical procedure and harsh conditions that reduce the irreproducibility of molecular imprinting. In the "grafting to" technique, imprinting polymerization was directed by the end vinyl groups located at particles' surface to form the MIPs layer at substrate. The process could be completed easily through simple free radical polymerization. However, the most disadvantage of "grafting to" method is low grafting densities [32,33]. In order to increase the graft efficiency, several means have been adopted, for instance, controlled radical polymerization (CRP) techniques [34,35] and isolated reactive sites at the surface of nanoparticles with protecting groups to depress steric crowding [36]. As a result, the grafting densities are improved but the process becomes complex and uncontrollable. Thus, the further development of the "grafting to" molecular imprinting technique at the surface of adsorbents such as silica particles by a simple/reliable method remains a challenge.

In this work, we report a simple and straightforward strategy for coating MIPs layer at the surface of silica nanoparticles with a controllable shell thickness by tuning the amount of surface end vinyl groups (Fig. 1). The CP was first preassembled to noncovalent complex with methacrylic acid (MAA) due to the strong hydrogen bonds effect. The γ-methacryloxypropyltrimethoxysilane (γ-MAPS) was modified onto the surface of silica nanoparticles to produce the end vinyl bonds that acted as reactive sites to induce the selective occurrence of imprinting polymerization at the particle's surface. It has been demonstrated that the amount of end vinyl bonds can be adjusted to control the thickness of imprinted shell. With an optimal shell thickness, a large capacity, high selectivity and fast kinetics of binding target CP were achieved. Meanwhile, a novel analysis method of CP pesticide, based on dispersive MIP solid-phase extraction (dMIP-SPE) coupled with HPLC has been established for efficient separation and fast enrichment of CP from the complex matrix such as green vegetables, cucumber, pear and jujube.

2. Experimental

2.1. Reagents

Tetraethylorthosilicate (TEOS), γ-methacryloxypropyltrimethoxysilane (γ-MAPS), ethylene glycol dimethacrylate (EGDMA), chlorpyrifos, profenofos (PF), triazophos (TZ) and phoxim (PX) were purchased from Sigma-Aldrich (St. Louis, USA). Methacrylic acid, benzoyl peroxide (BPO) and 2,2′-azobisisobutyroni-trile (AIBN) from Shanghai Chemical Plant (Shanghai, China) were purified through recrystallization prior to use. Methanol of HPLC grade was purchased from Merck (Darmstadt, Germany). All other chemicals used were of analytical reagent grade.

2.2. Instrumentation and analytical conditions

A Bruker Vector 27 FT-IR spectrometer (Bruker, Ettlingen, Germany) with a resolution of 2 cm^{-1} and a spectral range of 4000–500 cm^{-1} was employed to examine infrared spectra of samples by a pressed tablet (sample: KBr = 1: 14 in mass). Thermal analysis of the imprinted nanoparticles was performed using a thermogravimetric analyzer (TGA, Model TGA-2050, TA Instruments) to determine the weight loss (wt.%). Measurements generally on samples of 10–15 mg contained in a platinum crucible were carried out in an airflow rate of 90 mL/min by a controlled 10 °C/min heating rate from 50 to 800 °C. An IKA Vortex Genius 3 homogenizer (IKA, Staufer, Germany) was applied during the binding experiment. Transmission electron microscope (TEM) images were obtained by using a JEM-1010 transmission electron microscope at 80 kV (JEOL, Tokyo, Japan). The amount of CP was analyzed by HPLC system (Shimadzu, Kyoto, Japan) equipped with LC-10ATvp pump, SPD-10Avp detector, CTO-10ASvp column oven and Shimadzu shim-pack C_{18} column (5 μm, 250 mm × 4.6 mm i.d.). The mobile phase was methanol-water (98/2, v/v) at flow rate of 1.0 mL/min. All sample solutions were filtered through a 0.45 μm membrane before injection. The injection volume was 20 μL and the detection was carried out at 240 nm.

2.3. Preparation and chemical modification of silica nanoparticles

Monodispersed spherical silica nanoparticles were prepared by the hydrolysis of TEOS [37] with aqueous ammonia according to the single step process [38–40]. First, ammonia (9 mL) was dissolved in ethanol (50 mL), then the mixture of TEOS (5 mL) in ethanol (30 mL) was added with a constant flow rate and stirred at room temperature for 24 h. After centrifugation, the silica nanoparticles were refluxed in 10% HCl solution for 12 h and dried in vacuum at 120 °C before used. Next, the obtained silica nanoparticles (500 mg) and γ-MAPS (10 mL) were dispersed in dry toluene (50 mL) and stirred under nitrogen at 50 °C for 24 h. The mixture was centrifuged and the modified silica nanoparticles (SiO_2-MAPS) were rinsed with toluene, dried under vacuum at room temperature.

2.4. Determination of double bonds at the surface of silica nanoparticles

The amount of double bonds at the surface of silica nanoparticles was determined based on the catalytic bromine addition. Typically, 37 mL of HAc, 76 mL of CCl_4, 61 mL of CH_3OH, 9 mL of H_2SO_4/H_2O (1/5, v/v), and 7 mL of 10% $HgCl_2/CH_3OH$ (m/v) were added to make 190 mL of solvent mixture. To obtain organic phase of under layer as addition reaction medium, the solvent mixture was shaken uniformly and placed under steady-state for demixing. At this point, the solution of under layer mainly contains CCl_4, CH_3OH, $HgCl_2$ and so on. Subsequently, 10 mL of the solution of under layer, 150 mg of SiO_2-MAPS particles, 50 mL of 0.1 mol/L $KBrO_3$/KBr solution, and 2 mL of concentrated hydrochloric acid were added into a 250 mL Erlenmeyer flask. The flask was stuffed with stopper, shaken uniformly, and stored in a dark place for 25 min. In above process, the reaction of $KBrO_3$ and KBr produced Br_2 under acidic conditions. Then an addition reaction would occur between Br_2 and the double bonds at the surface of silica nanoparticles catalyzed by $HgCl_2$. After that, 1.5 g of KI was dissolved into the above solution and stored in a dark place for 5 min. Finally, the mixed solution was titrated with 0.1 mol/L $Na_2S_2O_3$ standard solution, and 0.5% starch solution was used as an indicator. The blank experiment was also done as described above but without the addition of SiO_2-MAPS particles. The experiments were repeated three times.

2.5. Imprinting of CP molecules at the surface of SiO_2-MAPS

CP-imprinted nanoparticles were prepared via free radical polymerization of template–monomer complex and cross-linking agent at the surface of SiO_2-MAPS. Typically, MAA (1.7 mmol) and CP (0.68 mmol) were dispersed in 30 mL mixture solvent with acetonitrile and toluene (3/1, v/v), placed for 12 h at low temperature

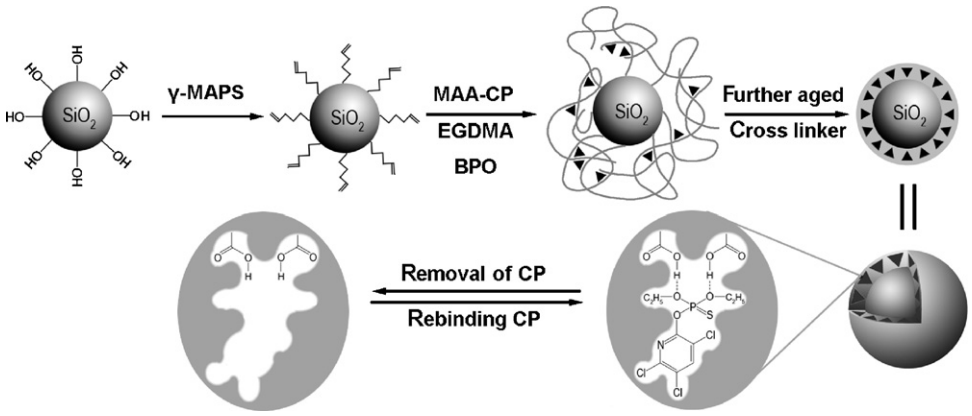

Fig. 1. Schematic illustration for the formation mechanism of CP-imprinted nanoparticles.

(4 °C), then followed by adding into 20 mL mixture solution including SiO_2-MAPS nanoparticles (100 mg), EGDMA (6.8 mmol) and BPO (40 mg), which were dispersed in the mixture solvent with acetonitrile and toluene (3/1, v/v) by ultrasonic vibration prior to use. Under nitrogen, the prepolymerization was first done at 50 °C for 6 h, polymerization at 60 °C for 24 h and further aged at 85 °C for 6 h. After centrifugation, the resultant composite nanoparticles were rinsed with acetonitrile and methanol. To remove template molecules from the polymer shell, the composite nanoparticles were extracted with a mixing CH_3OH/HAc solvent (9/1, v/v) in Soxhlet extractor for 1 h, then rinsed with methanol and dried under vacuum at room temperature.

The nonimprinted nanoparticles were also prepared using an identical procedure, but only in the absence of CP templates.

2.6. Rebinding experiment

Steady-state binding capacity of nanoparticles to CP was measured by suspending 20 mg of nanoparticles in 5 mL of chloroform with different CP concentrations (0.1–10 mmol/L). After the samples were incubated on a rocking table at room temperature for 12 h, the nanoparticles were separated from the solution phase through a 0.22 μm microporous membrane. The bound amount of CP in nanoparticles was determined by measuring the difference between total CP amount and residual amount in solution with HPLC. Meanwhile, the binding kinetics was tested by detecting the temporal evolution of CP concentration in the solutions. The molecular selectivity of the imprinted nanoparticles was investigated using the structure analogous PF, PX and TZ as compound competitors with CP.

2.7. Analysis of CP in spiked samples

Green vegetables, cucumber, pear and jujube were selected for the spiked samples. The edible parts of the samples were taken and crushed into homogenate before used. Sample homogenates (100 g) of green vegetables, cucumber, pear and jujube were mixed with 1 mL of CP standard solution (0.05 mg/mL), respectively, placed for 4 h, followed by adding into acetonitrile (100 mL) and stirred for 5 h before filtered. The filtrate was extracted with equal volume of chloroform and evaporated to dryness, then the residue was re-dissolved in 50 mL of chloroform to form the spiked samples solution.

CP-imprinted/nonimprinted nanoparticles (20 mg) were dispersed in the spiked sample solutions (5 mL) and incubated for 30 min. The nanoparticles were collected through a 0.22 μm microporous membrane, cleared up with chloroform (2 mL), and then dispersed in 1 mL of methanol/acetic acid (9/1, v/v). After incubation for 1 h, the nanoparticles in the desorption solution were separated through 0.22 μm microporous membranes. The desorption solution was dried by nitrogen and re-dissolved in methanol (1 mL). The obtained solutions were analyzed with HPLC. The reproducibility (between-assay precision) was based on six separate runs.

3. Results and discussion

3.1. Preparation and characterization of silica nanoparticles

Normally, silica nanoparticles have a high surface-to-volume ratio, heat resistance, corrosion resistance and do not swell in organic solvents, so they are widely used as support materials. Uniform silica nanoparticles with the size of 100–200 nm were usually prepared by the hydrolysis of TEOS with aqueous ammonia [37] and separated from the solution by centrifugation in the experiment. However, the centrifugation process should take a long time. In order to achieve rapid separation, the large-size silica nanoparticles were needed in our experiment. To obtain this kind of silica nanoparticles, there were two methods that could be adopted. One was single step process [39,40] and the other was seed particles growth process [41]. Taking into account whether to form the homogeneous and stable large-sized particles, the single step process was finally implemented, in which one reactant (TEOS/EtOH) was added into a reactor containing the other ones (H_2O/NH_4OH/EtOH) at a constant rate. When the flow rate kept at 5 μL/s, the results showed that the monodispersed and uniform spherical silica nanoparticles about 350 nm could be obtained. The silica nanoparticles can allow filtration through 0.22 μm microporous membranes to replace the centrifugation step in a convenient and fast way, as can be observed in Fig. 2.

3.2. Characterization of γ-MAPS agent modified silica nanoparticles

To coat the surface of silica particles with functional polymers, the vinyl functional monomers were immobilized at the surface of silica particles, followed by initiating a polymerization reaction of organic monomers. In this process, γ-MAPS was used as vinyl functional monomer. From the chemical structure, a conjugated system occurs in γ-MAPS where atoms covalently bond with alternating single and multiple bonds (O=C–C=C) and influence each other to produce a region called electron delocalization. Due to the strong electron attracting power of the carbonyl, it induces the high electron density at the O of the C=O and the low electron density of the conjugated C=C, leading to electrophilic character at the terminal alkene C. While, free radical polymerization is a nucleophilic

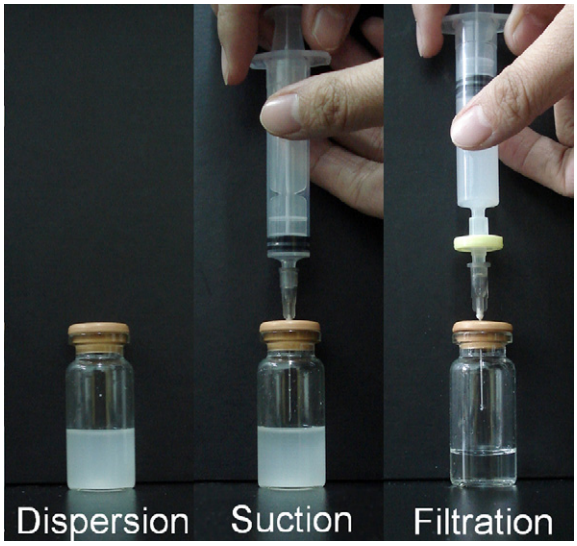

Fig. 2. Photos of dispersion, suction and filtration of nanoparticles.

reaction. These make that the polymerization between γ-MAPS and other vinyl functional monomers is easy.

The formation of SiO_2-MAPS was confirmed by the FT-IR measurements as shown in Fig. 3. Compared with the infrared data of pure silica (a), the SiO_2-MAPS (c) displayed clearly the characteristic peaks of γ-MAPS (b) including the C=O peaks at 1710 cm^{-1} and the relatively strong bands at the range of 2800–3000 cm^{-1} corresponded to the stretching vibration of C–H bonds to the methyl (or methylene) groups for γ-MAPS.

Meanwhile, the amount of double bonds at the surface of silica nanoparticles was determined through catalytic bromine addition. The addition reaction occurred between Br_2 (produced by the reaction of $KBrO_3$ and KBr under acidic conditions) and the double bonds at the surface of silica nanoparticles catalyzed by $HgCl_2$, and the excessive Br_2 was consumed by KI to form I_2, which could be quantitated through titrating with $Na_2S_2O_3$, and the starch solution was used as an indicator. The theory of the experiment can be summarized by following chemical equations:

$$KBrO_3 + 5KBr + 6HCl \rightarrow 3Br_2 + 6KCl + 3H_2O \quad (1)$$

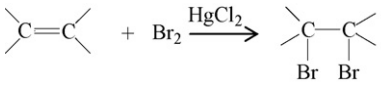

(2)

$$Br_2 + 2KI \rightarrow I_2 + 2KBr \quad (3)$$

$$I_2 + 2Na_2S_2O_3 \rightarrow 2NaI + Na_2S_4O_6 \quad (4)$$

The concentration of the double bonds at the surface of silica nanoparticles is used to evaluate the graft efficiency, and can be defined as:

$$E = \frac{(V_b - V_s)C}{2m} \quad (5)$$

Where E is the concentration of the double bonds at the surface of silica nanoparticles (μmol/g), V_b is the volume of $Na_2S_2O_3$ standard solution consumed in the blank experiment (L), V_s is the volume of $Na_2S_2O_3$ standard solution consumed in the sample experiment (L), C is the concentration of $Na_2S_2O_3$ standard solution (μmol/L), and m is the mass of silica nanoparticles (g).

Silica nanoparticles (0.5 g) were mixed with γ-MAPS at 5, 10, 15, 20 or 25 mL in 50 mL toluene solvent, prepared into SiO_2-MAPS 1, SiO_2-MAPS 2, SiO_2-MAPS 3, SiO_2-MAPS 4 and SiO_2-MAPS 5, respectively. And the concentration of the double bonds at the surface of silica nanoparticles was calculated by Eq. (5). The measurement results were shown in Fig. 4, which illustrated that the contents of double bonds at the silica nanoparticles surface rose with the addition of γ-MAPS.

3.3. Optimization of surface-imprinting synthesis conditions

The binding capacity for CP was extremely dependent on the amount of recognition sites in the MIPs layer, which was mainly affected by the surface polymerization. While, the grafting yield of γ-MAPS and initiator played an important part in the surface polymerization process. In order to study the influence of the grafting yield of γ-MAPS on the followed surface polymerization, SiO_2-MAPS 1, SiO_2-MAPS 2, SiO_2-MAPS 3, SiO_2-MAPS 4 and SiO_2-MAPS 5 were adopted and prepared into SiO_2@CP-MIP 1, SiO_2@CP-MIP 2, SiO_2@CP-MIP 3, SiO_2@CP-MIP 4 and SiO_2@CP-MIP 5, respectively, which was according to Section 2.5 and chose AIBN as initiator. The results of bound amount were shown in Fig. 5.

As can be seen from Fig. 5, the bound amount of SiO_2@CP-MIP 2 was the highest among the SiO_2@CP-MIPs. The result indicated that there were more recognition sites in SiO_2@CP-MIP 2 than that in other SiO_2@CP-MIPs.

Generally, the copolymers which were formed through the polymerization of template–monomer complexes and cross-linking agent, have three-dimensional space. At the surface of SiO_2-MAPS 2, the appropriate amount of vinyl groups induced the selective and high efficient occurrence of imprinting polymerization at the surface of silica nanoparticles, leading to form thick MIPs layer at the surface of silica nanoparticles after further aged, which contained so many recognition sites (Fig. 6b). However, at the surface of SiO_2-

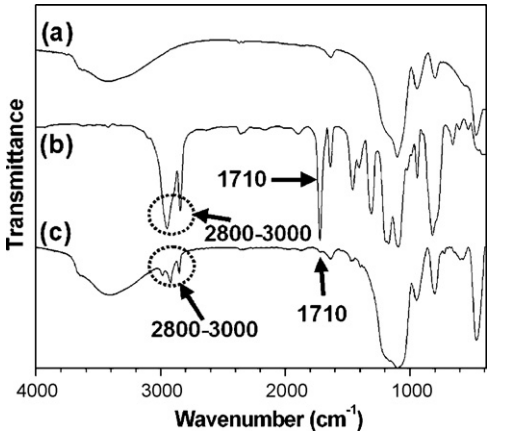

Fig. 3. The FT-IR spectra of (a) SiO_2, (b) γ-MAPS, and (c) SiO_2-MAPS.

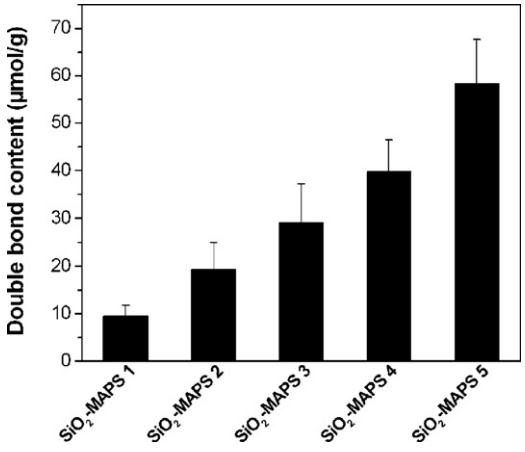

Fig. 4. The double bond contents at the surface of silica nanoparticles.

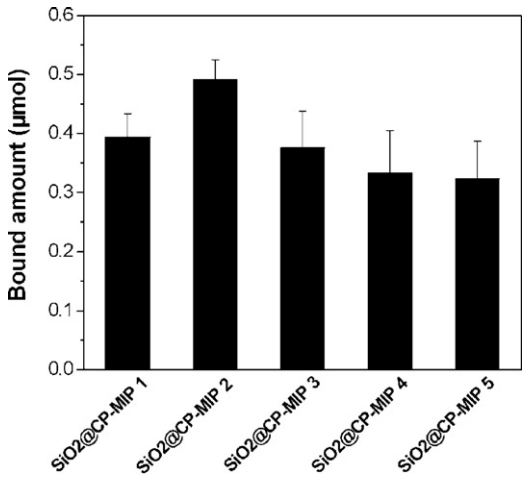

Fig. 5. The amounts of rebinding CP molecules by CP-imprinted nanoparticles with different surface vinyl groups at cores. The bound amounts were evaluated by suspending 20 mg nanoparticles in 5 mL solution, in which the concentration of CP was 1 mmol/L. Before the measurement, the sample was incubated for 12 h at room temperature on a homogenizer.

MAPS 1, the less amount of vinyl groups led to the low efficient occurrence of imprinting polymerization at surface of the particles, making thin MIPs layer which contained a few recognition sites (Fig. 6a). On the contrary, the vinyl groups were so crowded at the surface of SiO_2-MAPS 3 that the excessive amount of vinyl groups resulted in a low efficient occurrence of imprinting polymerization due to the possible inefficacy or self polymerization of surface vinyl groups, as indicated with hollow arrow or stuffed arrow in Fig. 6c, reducing the directing ability to the polymerizing reaction. Finally, the thickness of MIPs layer at the surface of SiO_2-MAPS 3 was also thin which led to a few recognition sites in the layer and low binding capacity. The situations of SiO_2@CP-MIP 4 and SiO_2@CP-MIP 5 were the same as that of SiO_2@CP-MIP 3.

By TEM observation (Fig. 7), the thicknesses of imprinted layer at the surface of SiO_2-MAPS 1, SiO_2-MAPS 2 and SiO_2-MAPS 3 are about 18 nm, 25 nm, 20 nm, respectively. Accordingly, as shown in Fig. 5, the bound amounts for CP of SiO_2@CP-MIP 1, SiO_2@CP-MIP 2, SiO_2@CP-MIP 3 are 0.3940 μmol, 0.4914 μmol, 0.3758 μmol, respectively. The results indicated that the thicker the layer is, the higher binding capacity is. Additionally, Fig. 8 is a two-stage mass loss curve in the temperature range of 50–800 °C. The first regime decrease below 100 °C is responsible for the removal of physically adsorbed water and solvent residues. In a successive heating from 100 to 700 °C, the steep decrease is attributed to the thermal decomposition of imprinted layer. And the weights (wt.%) of imprinted layer of SiO_2@CP-MIP 1, SiO_2@CP-MIP 2, SiO_2@CP-MIP 3 are about 11.8%, 15.8%, 13.6%, respectively. All of these are in agreement with the explanation on the Fig. 6. Thus, the results suggested that 10 mL of γ-MAPS was the optimal grafting amount.

Normally, the initiator plays a critical role in the forming copolymer and grafting process. With the extension of copolymers chain in the free radical polymerization, the activity of free radicals was declined, which would influence the ability to initiate vinyl polymerization. In addition, when AIBN was used as initiator, the occurrence of chain transfer reaction to monomer or solvent was

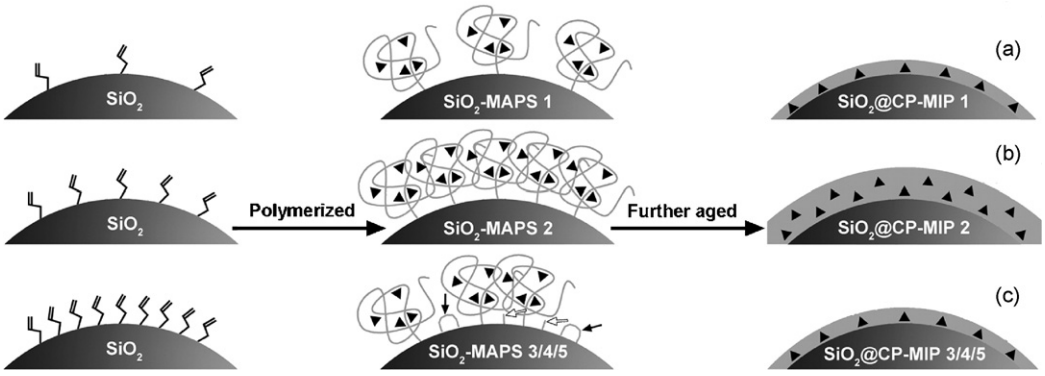

Fig. 6. Outline of fixation of different amount of γ-MAPS at silica nanoparticles and the coating MIP layer at silica nanoparticles via free radical polymerization. (a) SiO_2@CP-MIP 1, (b) SiO_2@CP-MIP 2, and (c) SiO_2@CP-MIP 3/4/5.

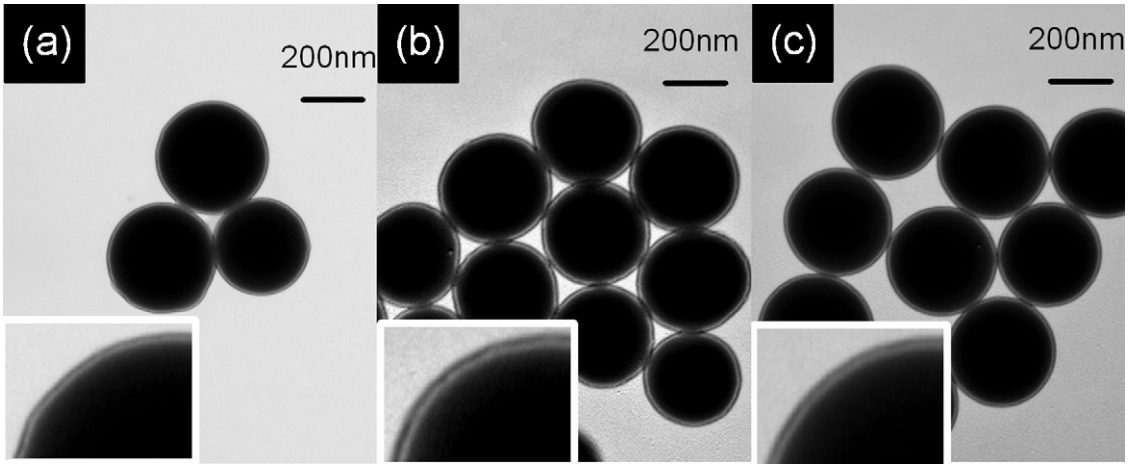

Fig. 7. TEM images of (a) SiO_2@CP-MIP 1, (b) SiO_2@CP-MIP 2, and (c) SiO_2@CP-MIP 3.

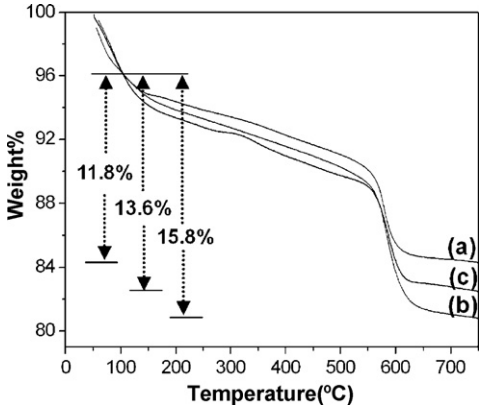

Fig. 8. Thermogravimetic weight loss curves of (a) SiO_2@CP-MIP 1, (b) SiO_2@CP-MIP 2, and (c) SiO_2@CP-MIP 3.

frequent. While BPO was used as initiator, the chain transfer to BPO was considerably increased, which led to produce new free radical. In order to maintain the activity of free radicals, our group used peroxidate initiator (BPO) instead of azo initiators (AIBN) to regulate radical polymerization.

Table 1 lists the bound amount of the SiO_2@CP-MIP 2/SiO_2@CP-NMIP 2 and SiO_2@CP-MIP 6/SiO_2@CP-NMIP 6. 20 mg of the SiO_2@CP-MIP 2 and SiO_2@CP-MIP 6 can most absorb 0.4914 and 0.9966 μmol of CP at equilibrium condition, respectively. Thus, the rebinding capacity of SiO_2@CP-MIP 6 is about 2.0-folds that of SiO_2@CP-MIP 2. The result indicated that BPO could improve polymerization efficiency, leading to make more recognition sites in the MIPs layer at the surface of silica nanoparticles than AIBN.

3.4. Molecular recognition property

To evaluate the molecular recognition properties of imprinted nanoparticles, the nonimprinted nanoparticles as a control sample were also synthesized under the same conditions, but only in the absence of CP templates, and commonly imprinted particles with a size of ~2 μm were synthesized by common free radical polymerization in the absence of silica mother particles.

The uptake amounts of CP by the imprinted/nonimprinted nanoparticles and the commonly imprinted particles were determined by measuring the difference between the total CP amount and the residual amount in the solution with HPLC. Fig. 9A shows that the amounts of binding CP by imprinted/nonimprinted nanoparticles and the commonly imprinted particles. 20 mg of the CP-imprinted, nonimprinted nanoparticles and commonly imprinted particles can most absorb 2.84, 0.79, and 1.43 μmol of CP at equilibrium condition, respectively. Thus, the rebinding capacity of CP-imprinted nanoparticles is about 3.6- and 2.0-folds that of nonimprinted and commonly imprinted particles, respectively.

Table 1
Comparison of the imprinting effect of nanoparticles.

Nanoparticles	Modified silica	Initiator	Bound (μmol)[a]	α (K_i/K_n)[b]
SiO_2@CP-MIP 2	SiO_2-MAPS 2	AIBN	0.4914	1.933
SiO_2@CP-NMIP 2	SiO_2-MAPS 2	AIBN	0.2542	
SiO_2@CP-MIP 6	SiO_2-MAPS 2	BPO	0.9966	2.221
SiO_2@CP-NMIP 6	SiO_2-MAPS 2	BPO	0.4488	

[a] The binding amount of different nanoparticles were evaluated by suspending 20 mg nanoparticles in 5 mL solution, in which the concentration of CP was 1 mmol L^{-1}. Before the measurement, the sample was incubated for 12 h at room temperature on a homogenizer.

[b] K_i and K_n are the partition coefficients of analytes on imprinted and nonimprinted particles, respectively. The α is the imprinting factor of analytes, defined as K_i/K_n. K = [(moles of test compound bound to imprinted material)/(g of imprinted material)]/[(moles of test compound bound remaining in solution)/(g of solution)].

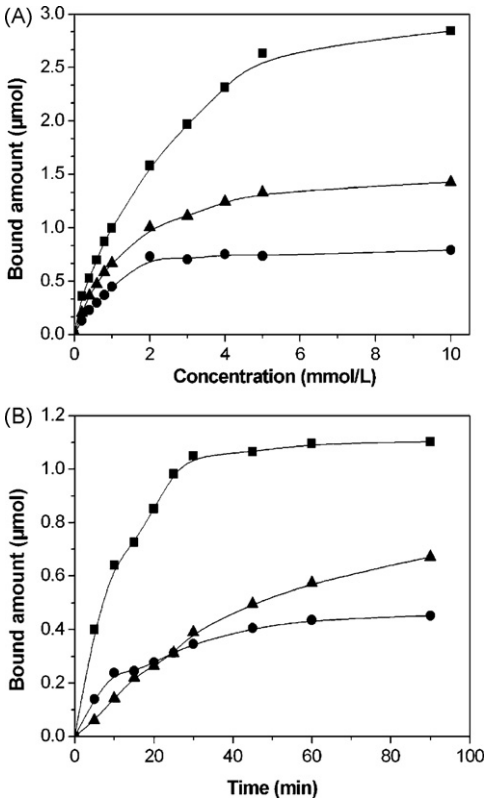

Fig. 9. The comparisons of molecular recognition properties. (A) The rebinding amount and (B) the kinetic uptake of CP molecules by (■) CP-imprinted nanoparticles, (▲) commonly imprinted particles and (●) nonimprinted nanoparticles. The amounts of rebinding CP were measured by suspending 20 mg of imprinted materials in 5 mL of solution with different CP concentrations. The data of binding kinetics were obtained using 1 mmol/L CP solution.

Binding kinetics of the template CP with imprinted/nonimprinted nanoparticles and the commonly imprinted particles were also evaluated. Fig. 9B shows the adsorption CP versus the incubation time. Before adsorption equilibrium was reached. The imprinted/nonimprinted nanoparticles required a shorter time (30 min) than did the commonly imprinted particles (90 min).

These measurements show that the density of effective imprinted sites in the imprinted nanoparticles is much higher than that in commonly imprinted particles. In the case of commonly imprinted particles, those original templates situated at the central area of bulky particles cannot completely be removed from the cross-linked rigid matrix. Moreover, the deep imprinted sites are difficultly accessed by target analyte due to the high mass-transfer resistance. Only these imprinted sites in the proximity of the particles' surface are effective for rebinding target analyte. These make commonly imprinted particles exhibit both lower binding capacity and slower kinetics than the imprinted nanoparticles with a thin shell.

3.5. Molecular selectivity of the CP-imprinted nanoparticles

The molecular selectivity of imprinted nanoparticles was measured using the structure-analogous PF, TZ and PX as compound competitors with CP in the mixture solution. As shown in Fig. 10, the rebinding capacities of the imprinted nanoparticles to CP are

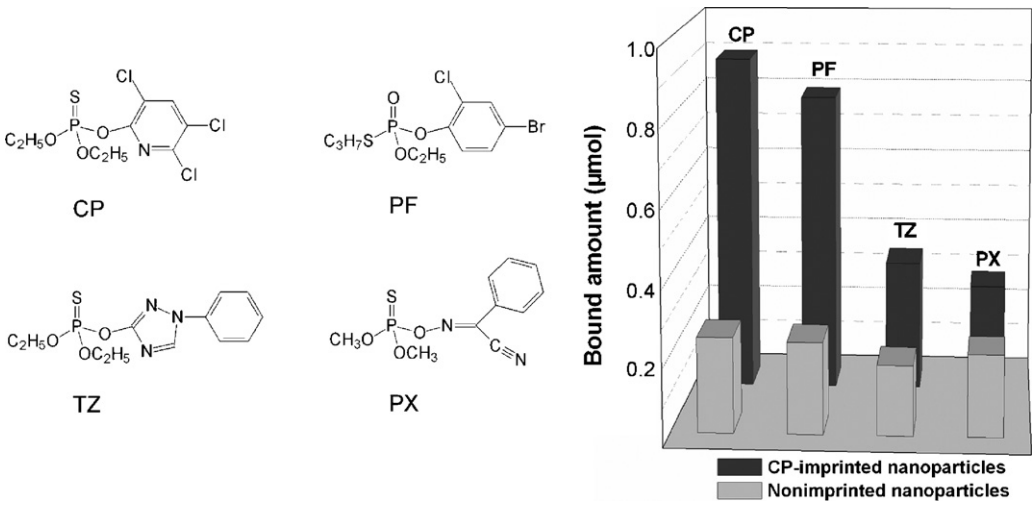

Fig. 10. The molecular selectivity of the CP-imprinted nanoparticles and nonimprinted nanoparticles. The measurements were carried out by suspending 20 mg of samples in 5 mL of mixed solution, in which the concentrations of CP, PF, TZ and PX were 1 mmol/L, respectively. Before the measurement, the samples were incubated for 30 min at room temperature on a homogenizer.

about 1.1-, 2.6- and 3.1-folds that to PF, TZ and PX, respectively. However, the nonimprinted nanoparticles do not exhibit the obvious difference in the rebinding capacities of CP, PF, TZ and PX. From the chemical structure, the PF molecules possess almost approximate molecular dimension and functional group with CP, which could make PF enter into the imprinted cavities of CP easily. Therefore, CP-imprinted nanoparticles exhibit a large binding affinity to PF similar to CP, which is higher than the nonimprinted nanoparticles. Although TZ and PX molecules also have phospholipid groups, the mismatch of their structure and size with CP-imprinted cavities may greatly hinder them from entering into the imprinted cavities, leading to the lower binding capacities. Thus, the small binding capacities of TZ and PX are mainly attributed to the nonspecific binding, which also leads to a very small difference of binding affinities between imprinted and nonimprinted nanoparticles (Fig. 10). These comparisons clearly demonstrate the CP-imprinted layers at the surface of silica nanoparticles have high molecular selectivity for the target species.

3.6. Selective separation of CP from the spiked samples

The spiked sample of green vegetables, cucumber, pear and jujube were selected for validation of the CP-imprinted nanoparticles' selectivity. Fig. 11a is the HPLC chromatogram of complex spiked samples containing 1 μg/mL of CP, in which the complexity of the spiked sample background is evident. Compared with the direct HPLC analysis (Fig. 11a), the interference in four spiked samples are successfully cleaned up after extracted with CP-imprinted nanoparticles (Fig. 11b), thus allowing the extraction of CP with high selectivity. The average recoveries were 76.1%, 78.4%, 82.9%, 93.5% and the RSDs were 3.6%, 6.8%, 4.6%, 9.7%, respectively. On the contrary, the nonimprinted nanoparticles showed no such selectivity (Fig. 11c). The results demonstrated that the CP-imprinted nanoparticles had high selectivity and enrichment ability. Hence, the CP-imprinted nanoparticles offer itself as a simple and straightforward technique for the direct analysis of CP from the complicated matrices without lengthy sample cleanup.

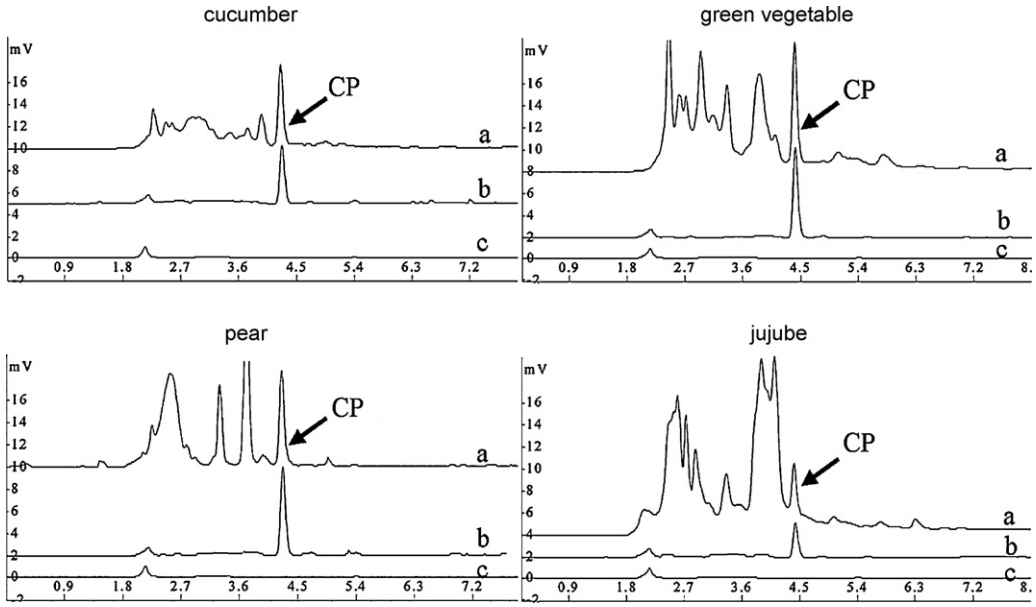

Fig. 11. HPLC chromatograms of (a) spiked sample solution containing 1 μg/mL CP, (b) spiked sample solution extracted with CP-imprinted nanoparticles, and (c) spiked sample solution extracted with nonimprinted nanoparticles.

4. Conclusions

In summary, we have developed the use of tuning of the vinyl groups' spacing at surface of modified silica to coat the thick molecular imprinted polymers layer at the silica nanoparticles' surface. The average thickness of MIPs layer was ~25 nm. The resultant CP-imprinted nanoparticles exhibited good characteristics, such as highly spherical and uniform morphology, good reproducibility, high binding capacity and quick kinetics for the rebinding of CP. The combination of dMIP-SPE and HPLC makes it possible that selective determination of the trace CP from complex matrices can be easily carried out. Therefore, the approach described here will provide new opportunities in the applications involved in the highly selective separation and fast enrichment of pesticides from complicated matrices.

Acknowledgments

This work is supported by the National 863 High Technology Project of China (Nos. 2008AA10Z421 and 2007AA10Z434), the National Natural Science Foundation of China (Nos. 30801558, 20807042, and 20925518), Program of Jiangsu Provincial 6th Session Talent Summit (No. 07-C-009), China-Singapore Joint Research Project (2009DFA51810) and Innovation Project of Chinese Academy of Sciences (KSCX2-YW-G-058).

References

[1] S. Zhang, H. Zhao, R. John, Biosens. Bioelectron. 16 (2001) 119.
[2] S. Fennouh, V. Casimiri, C. Burstein, Biosens. Bioelectron. 12 (1997) 97.
[3] C. Cremisini, S. Disario, J. Mela, R. Pilloton, G. Palleschi, Anal. Chim. Acta 311 (1995) 273.
[4] A. Guerrieri, L. Monaci, M. Quinto, F. Palmisano, Analyst 127 (2002) 5.
[5] A. Cappielo, G. Famiglini, P. Palma, F. Mangani, Anal. Chem. 74 (2002) 3547.
[6] S. Lacorte, D. Barcelo, Anal. Chem. 68 (1996) 2464.
[7] J.C. Xie, L.L. Zhu, H.P. Luo, L. Zhou, C.X. Li, X.J. Xu, J. Chromatogr. A 934 (2001) 1.
[8] X.C. Dong, W. Wang, S.J. Ma, H. Sun, Y. Li, J.Q. Guo, J. Chromatogr. A 1070 (2005) 125.
[9] H. Li, Y.G. Liu, Z.H. Zhang, H.P. Liao, L.H. Nie, S.Z. Yao, J. Chromatogr. A 1098 (2005) 66.
[10] S.G. Hu, L. Li, X.W. He, J. Chromatogr. A 1062 (2005) 31.
[11] F. Chapuis, J.U. Mullot, V. Pichon, J. Chromatogr. A 1135 (2006) 127.
[12] J.J. Ou, L. Kong, C.S. Pan, X.Y. Su, X.Y. Lei, H.F. Zou, J. Chromatogr. A 1117 (2006) 163.
[13] F. Lanza, B. Sellergren, Anal. Chem. 71 (1999) 2092.
[14] L.I. Andersson, J. Chromatogr. B 745 (2000) 3.
[15] C.X. Zhai, Q. Lu, X.M. Chen, Y. Peng, L.N. Chen, S.H. Du, J. Chromatogr. A 1216 (2009) 2254.
[16] V. Pichon, F. Chapuis-Hugon, Anal. Chim. Acta 622 (2008) 48.
[17] K. Haupt, Anal. Chem. Mater. 75 (2003) 376.
[18] L. Ye, K. Mosbach, Chem. Mater. 20 (2008) 895.
[19] H.Q. Shi, W.B. Tsai, M.D. Garrison, S. Ferrari, B.D. Ratner, Nature 398 (1999) 593.
[20] O. Hayden, K.J. Mann, S. Krassnig, F.L. Dickert, Angew. Chem. Int. Ed 45 (2006) 2626.
[21] O. Hayden, P.A. Lieberzeit, D. Blaas, F.L. Dickert, Adv. Funct. Mater. 16 (2006) 1269.
[22] M. Tatemichi, M. Sakamoto, M. Mizuhata, S. Deki, T. Takeuchi, J. Am. Chem. Soc. 129 (2007) 10906.
[23] A. Bossi, S.A. Piletsky, E.V. Piletska, P.G. Righetti, A.P.F. Turner, Anal. Chem. 73 (2001) 5281.
[24] R.H. Schmidt, K. Mosbach, K. Haupt, Adv. Mater. 16 (2004) 719.
[25] S.C. Zimmerman, M.S. Wendland, N.A. Rakow, I. Zharov, K.S. Suslick, Nature 418 (2002) 399.
[26] C.J. Tan, Y.W. Tong, Anal. Bioanal. Chem. 389 (2007) 369.
[27] E. Yilmaz, K. Haupt, K. Mosbach, Angew. Chem. Int. Ed. 39 (2000) 2115.
[28] J. Pyun, K. Matyjaszewski, Chem. Mater. 13 (2001) 3436.
[29] N.P. Kyle, Z. Xi, S.M. Jeffrey, E.L. Deborah, Langmuir 22 (2006) 4259.
[30] M.M. Titirici, B. Sellergren, Chem. Mater. 18 (2006) 1773.
[31] S. Voccia, C. Jérôme, C. Detrembleur, Chem. Mater. 15 (2003) 923.
[32] Y. Lyatskaya, A.C. Balazs, Macromolecules 31 (1998) 19.
[33] B. Zhao, W.J. Brittain, Prog. Polym. Sci. 25 (2000) 677.
[34] J. Wen, G.L. Wilkes, Chem. Mater. 8 (1996) 1667.
[35] R.J.P. Corriu, Int. Ed. Engl. 39 (2000) 1376.
[36] J.C. Hicks, R. Dabestani, A.C. Buchanan, C.W. Jones, Chem. Mater. 18 (2006) 5022.
[37] W. Stöber, A. Finker, E.J. Bohn, Colloid Interface Sci. 26 (1968) 62.
[38] K. Nozawa, H. Gailhanou, L. Raison, Langmuir 21 (2005) 1516.
[39] (a) K.D. Kim, H.J. Bae, H.T. Kim, Colloids Surf. A 224 (2003) 119;
(b) K.D. Kim, H.T. Kim, Colloids Surf. A 207 (2002) 263.
[40] S.K. Park, K.D. Kim, H.K. Kim, J. Ind. Eng. Chem. 6 (2000) 365.
[41] S.M. Chang, M. Lee, W.S. Kim, Colloid Interface Sci. 286 (2005) 536.